

# The CDF II Level 1 Track Trigger Upgrade

A. Abulencia<sup>§</sup>, P. Azzurri<sup>||</sup>, W. Brian<sup>\*</sup>, E. Cochran<sup>¶</sup>, J.R. Dittmann<sup>\*</sup>, S. Donati<sup>||</sup>, J. Efron<sup>¶</sup>, R. Erbacher<sup>†</sup>, D. Errede<sup>§</sup>, I. Fedorko<sup>||</sup>, G. Flanagan<sup>\*\*</sup>, R. Forrest<sup>†</sup>, M. Frank<sup>\*</sup>, J. Gartner<sup>¶</sup>, H. Gerberich<sup>§</sup>, S. Hewamanage<sup>\*</sup>, S. Holm<sup>‡</sup>, R. Hughes<sup>¶</sup>, A. Ivanov<sup>†</sup>, M. Johnson<sup>¶</sup>, M. Jones<sup>\*\*</sup>, T. Junk<sup>§</sup>, M. Kasten<sup>§</sup>, B. Kilminster<sup>¶</sup>, R. Klein<sup>‡</sup>, N. Krumnack<sup>\*</sup>, K. Lannon<sup>¶</sup>, S. Levine<sup>§</sup>, A. Lister<sup>†</sup>, J. McKim<sup>¶</sup>, R. Mokos<sup>§</sup>, D. Olivito<sup>¶</sup>, B. Parks<sup>¶</sup>, K. Pitts<sup>§</sup>, E. Rogers<sup>§</sup>, E.E. Schmidt<sup>‡</sup>, L. Scott<sup>‡</sup>, T. Shaw<sup>‡</sup>, J. Slaunwhite<sup>¶</sup>, A. Soha<sup>†</sup>, A. Staveris<sup>||</sup>, G. Veramendi<sup>§</sup>, J.S. Wilson<sup>\*</sup>, P.J. Wilson<sup>‡</sup>, B. Winer<sup>¶</sup>

<sup>\*</sup> Department of Physics, Baylor University,  
One Bear Place 97316, Waco, TX 76798-7316

<sup>†</sup> Department of Physics, University of California,  
One Shields Avenue, Davis, CA 95616

<sup>‡</sup> Fermi National Accelerator Laboratory,  
P.O. Box 500, Batavia, IL 60510-0500

<sup>§</sup> Department of Physics, University of Illinois,  
1110 West Green, Urbana, IL 61801-3080

<sup>¶</sup> Department of Physics, Ohio State University,  
191 West Woodruff Ave, Columbus, OH 43210-1117

<sup>||</sup> Istituto Nazionale di Fisica Nucleare

Edificio C - Polo Fibonacci Largo B. Pontecorvo, 3, I-56127 Pisa, Italy

<sup>\*\*</sup> Department of Physics, Purdue University

525 Northwestern Ave, West Lafayette, IN 47907-2036

**Abstract**—The CDF II detector uses dedicated hardware to identify charged tracks that are used in an important class of level 1 trigger decisions. Until now, this hardware identified track segments based on patterns of hits on only the axial sense wires in the tracking chamber and determined the transverse momentum of track candidates from patterns of track segments. This identification is efficient but produces trigger rates that grow rapidly with increasing instantaneous luminosity. High trigger rates are a consequence of the large numbers of low momentum tracks produced in inelastic  $p\bar{p}$  collisions which generate overlapping patterns of hits that match those expected for high-momentum tracks. A recently completed upgrade to the level 1 track trigger system makes use of information from stereo wires in the tracking chamber to reduce the rate of false triggers while maintaining high efficiency for real high momentum particles. We describe the new electronics used to instrument the additional sense wires, identify track segments and correlate these with the track candidates found by the original track trigger system. The performance of this system is characterized in terms of the efficiency for identifying charged particles and the improved rejection of axial track candidates that do not correspond to real particles.

## I. INTRODUCTION

Since 2001, the CDF II detector has collected data used to carry out a rich physics program at the Fermilab Tevatron  $p\bar{p}$  collider. Many of the data samples used for the analysis of electroweak processes, the production and decay of top quarks and the decays of  $b$ - and  $c$ -hadrons rely on the identification of charged tracks in the level 1 trigger. These tracks are identified by the eXtremely Fast Tracker (XFT) system[1] using data

from axial sense wires in the central tracking chamber[2] and are extrapolated outward to the calorimeter and muon chambers to form lepton triggers at Level 1, or inward to the silicon detector to form triggers on tracks from displaced secondary vertices at Level 2[3].

Recently, upgrades to the Fermilab accelerator complex allow  $p\bar{p}$  collisions to be initiated with instantaneous luminosities that routinely exceed  $200 \times 10^{30} \text{ cm}^{-2}\text{s}^{-1}$ , producing an average of 6  $p\bar{p}$  interactions in each bunch crossing. The high detector occupancy from these inelastic collisions produces overlapping patterns of hits that are incorrectly identified as high momentum tracks, leading to trigger rates that grow rapidly with instantaneous luminosity. Without the use of additional information to increase the purity of these triggers, their rates were controlled by either raising thresholds or by prescaling triggers, resulting in significant loss of trigger acceptance and efficiency.

Here we describe an upgrade to the level 1 track trigger that makes use of information from the stereo wires in the tracking chamber to improve the purity of tracks found by the axial XFT system.

## II. THE AXIAL XFT SYSTEM

The upgraded track trigger system enhances, rather than replaces, the existing axial XFT system. Since both make use of data from the tracking chamber in similar ways, it is useful to provide an overview of the axial system which has been in operation for several years now. A block diagram of the axial

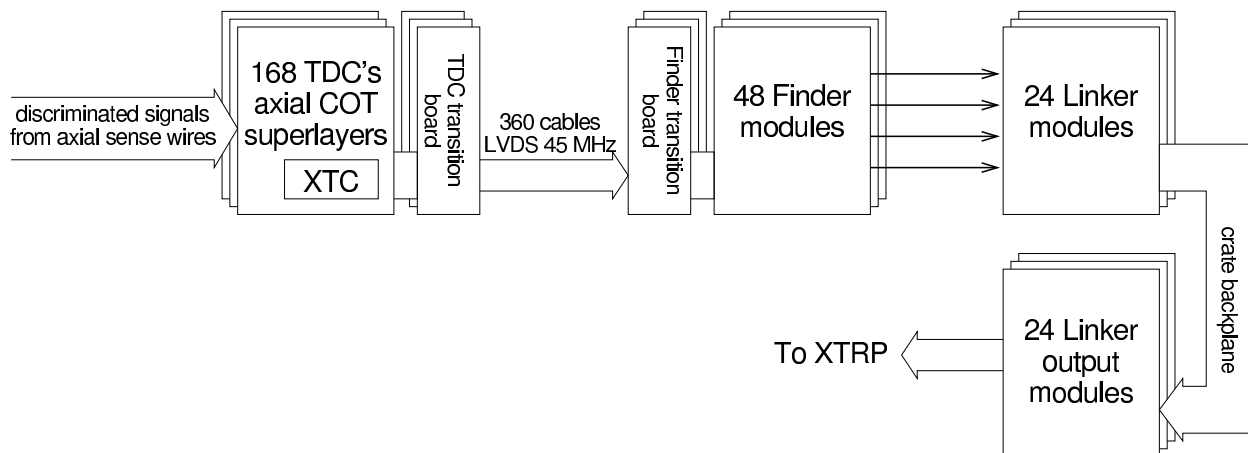


Fig. 1. Components of the axial XFT system. The XTRP system, which processes the data from the Linker Output Module, is not shown.

XFT system is shown in Figure 1, the components of which are described below.

#### A. Tracking Chamber

The CDF II tracking chamber has sense wires arranged in 8 super-layers in which the wire planes alternate between axial and  $2^\circ$  stereo. Drift cells in each super-layer have 12 sense wires located between field sheets and are all of approximately the same size. The maximum drift distance is about 9 mm resulting in a maximum drift time of approximately 177 ns when operated with an 50 : 50 mixture of Argon/Ethane. The innermost super-layer contains 168 stereo cells, while the outermost super-layer as 480 axial drift cells. Analog signals induced on each wire are read out using fixed threshold discriminators that encode the charge in the width of their digital output. Eight adjacent cells are read out 96-channel TDC modules which digitize the arrival times of their leading and and trailing edges with a precision of 1 ns.

#### B. XTC mezzanine board

Each axial sense wire provides two bits of drift time information to the level 1 track trigger system by way of a mezzanine board mounted on the TDC. As it was originally foreseen that the Tevatron could be operated with a 108 bunches of protons and anti-protons, two bits of drift time data per wire are transferred from the TDC modules mounted on the detector to the level 1 track trigger electronics using synchronous parallel LVDS signals every 132 ns. In practice, however, the Tevatron operates with 36 bunches and a 396 ns bunch crossing interval, and identical copies of the data from a valid bunch crossing are transferred in three consecutive 132 ns intervals.

#### C. Finder module

Data from the XTC mezzanine boards are received by Finder Modules, which identify cases in which hits in four adjacent cells are consistent with predefined patterns of hits corresponding to valid segments from tracks with  $p_T > 1.5$  GeV/c. Twelve bits of data referred to as “pixels” are

used to identify the azimuthal positions of valid track segments passing through cells in the inner two axial super-layers, while six groups of two bits are used in the outer two axial super-layers. The two bits at each azimuthal position provide a means to describe tracks with positive or negative curvature.

#### D. Linker module

Pixel data is sent from the Finders to Linker Modules which identify groups of pixels in the four super-layers that match predefined patterns corresponding to valid tracks. Each Linker module processes patterns of hits that could be produced from tracks with  $p_T > 1.5$  GeV/c within  $1.25^\circ$  azimuthal regions and associates 7 bits of curvature data and three bits of fine azimuthal data with the highest  $p_T$  track identified within each region. The axial XFT system also provides two additional bits to indicate whether a track is isolated or exits the chamber before passing through the outermost axial super-layer. The 12-bit words describing identified tracks are sent on the crate backplane to Linker Output Modules. These modules drive the information via a cable on the front panel to the XTRP system which extrapolates tracks to the outer sub-detectors.

### III. AXIAL XFT PERFORMANCE AT HIGH LUMINOSITY

The axial Finder modules set pixels corresponding to track segments with  $p_T$  as low as 1.5 GeV/c. Large numbers of pixel bits are set at high instantaneous luminosity due to the many low momentum tracks produced in inelastic  $p\bar{p}$  interactions. Figure 2 illustrates how tracks are correctly identified by the Linker modules when the occupancy is low, but at higher occupancies the large numbers of pixels produced by low momentum particles lead to tracks being incorrectly identified by the Linker. As a consequence of the high rate of “fake” tracks, level 1 triggers based on tracks found with the axial system have cross sections that grow rapidly with instantaneous luminosity.

As an example, we consider a class of triggers that identifies the presence of two tracks with requirements imposed on their transverse momentum, opening angle and the scalar sum of their transverse momenta. These are used to drive the level 2

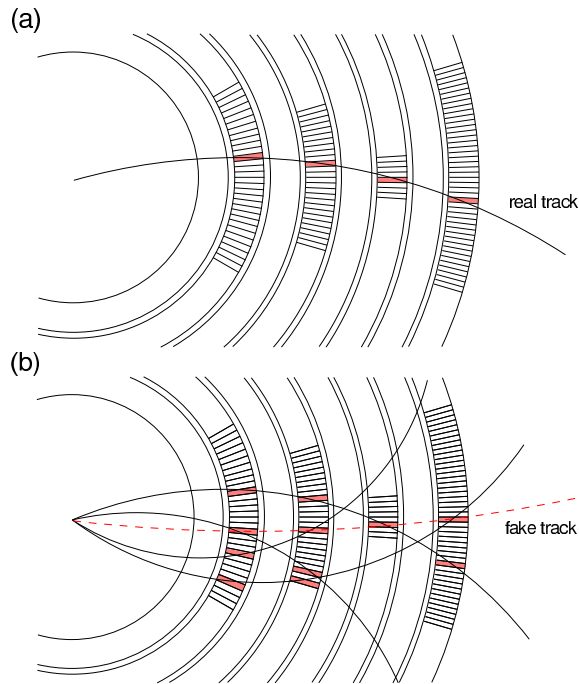


Fig. 2. Behavior of the Linker (a) at low and (b) at high occupancies. Filled cells indicate pixels matched by the finder. The dashed line in (b) indicates a fake track found in the pattern of overlapping pixels produced by overlapping low momentum tracks.

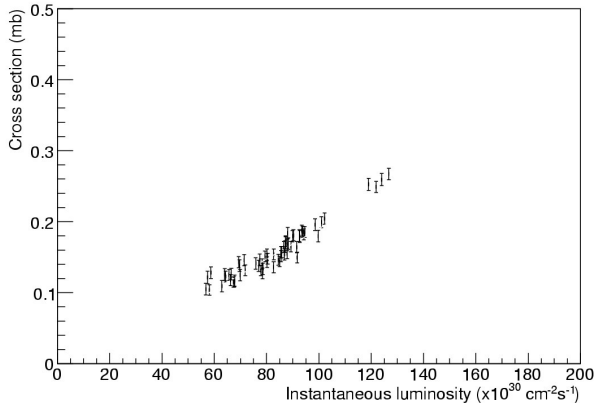


Fig. 3. Cross section as a function of instantaneous luminosity for the level 1 trigger requiring two tracks with  $p_T > 2.5$  GeV/c, opening angle less than  $90^\circ$  and scalar sum of their transverse momentum greater than 6.5 GeV/c.

triggers that associate silicon hits with the tracks and require the presence of displaced secondary vertices to select decays of  $b$ - and  $c$ -hadrons. Maintaining this trigger path was crucial for the CDF II heavy flavor physics program, including the observation of  $B_s^0$  oscillations[4], but its level 1 trigger cross section, shown in Figure 3, grows rapidly with instantaneous luminosity due to the growing rates of fake tracks found by the Linker. This trigger saturated the available level 1 trigger bandwidth at high instantaneous luminosities, making it necessary to impose trigger prescales at moderate luminosities and disabling the trigger when  $\mathcal{L} > 120 \text{ cm}^{-2}\text{s}^{-1}$ .

To study the behavior of the axial XFT system at high luminosity, an emulation of the trigger algorithms was applied to data with additional hits in the tracking chamber superimposed to replicate the effect of multiple  $p\bar{p}$  interactions. These studies indicated that when  $\mathcal{L} = 300 \times 10^{30} \text{ cm}^{-2}\text{s}^{-1}$ , 80% of the triggered events would have at least one fake track. The need to provide a higher purity sample of tracks selected by the XFT system for use in the level 1 trigger motivated the upgrade described here. The goals of the upgrade were to significantly reduce trigger rates by rejecting fake tracks found by the axial system, while maintaining high trigger efficiencies. Furthermore, the upgrade was to be installed and commissioned without significantly impacting data collection which relies heavily on the axial XFT trigger.

#### IV. XFT UPGRADE

The XFT upgrade makes use of data from wires in the the outer three stereo super-layers to confirm the presence of tracks found with the axial XFT system. Track segments are identified using hits in stereo super-layers and their spatial correlation with axial tracks is used to confirm the presence of real tracks. The upgrade was designed to make use of the 396 ns bunch crossing interval, allowing three times as much information to be transferred per wire at the same rate as is used in the axial system. Figure 4 shows the configuration of the axial XFT system and the new components of the system used in the upgrade. These consist of a new TDC mezzanine card, the Stereo Finder module and Stereo Linker Association Modules (SLAM), which replaces the Linker Output Modules.

##### A. TDC Interface

To fully exploit the increased time during which hit data could be sent from the TDC to the trigger electronics, a new mezzanine card (XTC2) was developed to interface with TDC's in the outer three axial super-layers. The XTC2 card reports hit times in 6 bins, the edges of which are controlled by VME registers on the TDC. Two overlapping sets of 6 time bits were implemented to provide logic which avoids cases in which a narrow pulse near a bin boundary could set bits in adjacent time bins. Six bits of timing information per wire are sent to a transition module in the back of the VME crate by way of the TDC motherboard and pass-through connectors on the crate backplane. The transition module receives 32 bits of timing data each 22 ns, reformats it and transfers it to a 4-channel fiber transmitter mezzanine board, designed according to the Common Mezzanine Card (CMC) standard[5]. This card was developed for upgrades of the level 2 trigger system[6] and is used elsewhere in the XFT upgrade. The fiber transmitter uses TLK1501[7] devices to serializes the data into 24-bit words which are transferred to Stereo Finder modules every 16.5 ns via approximately 150 feet of optical fiber.

##### B. Stereo Finder

The Stereo Finder modules identify track segments based on the data received from the TDC's that instrument the

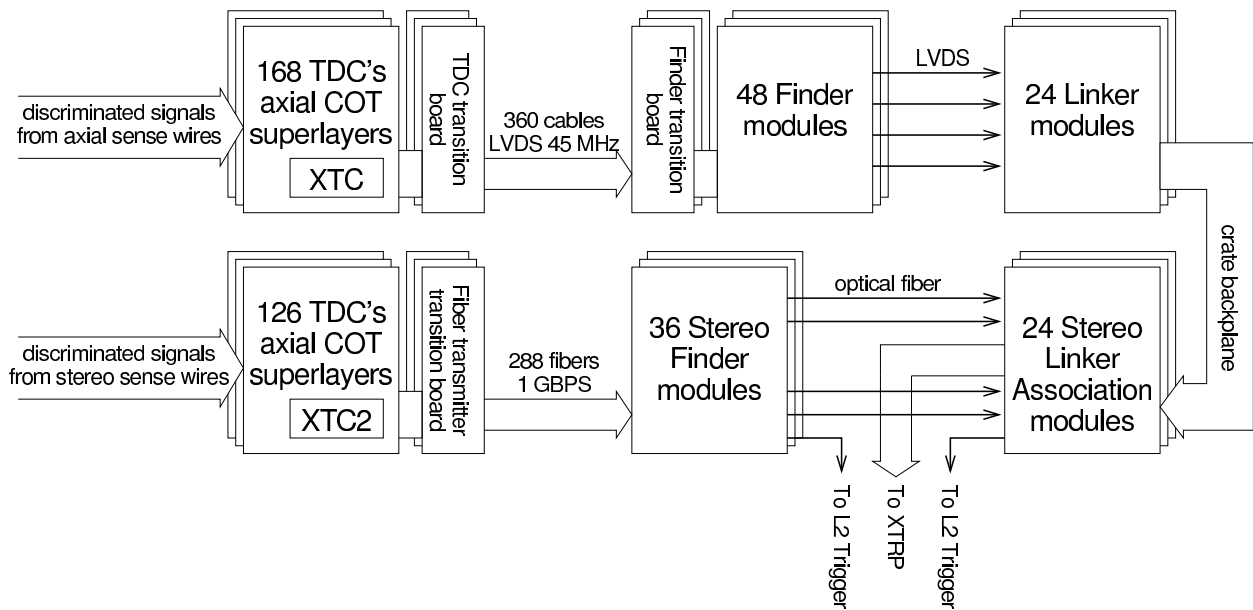


Fig. 4. Components of the upgraded XFT system. The XTRP system and the interface to the level 2 trigger system are not shown.

outer three stereo super-layers. Data from each super-layer are received by 12 stereo finder modules using 4-input optical receiver mezzanine boards and perform deserialization of the data stream using TLK1501 devices. Two Altera Stratix 2 EP2S60[8] FPGA's on each Stereo Finder module align the input data in FIFO macrocells and test the input data stream for hit patterns consistent with track segments.

In each 16.5 ns clock cycle, each finder FPGA examines data from 8 adjacent cells. Figure 5 illustrates the way in which hit data is processed to identify a track segment. The logic that associates valid track segments with hit data is specified using VHDL code generated by a program that identifies the most frequently used patterns of hits from tracks simulated with a uniform distribution of curvature and rapidity. Wires in each cell are divided into three groups of four wires to facilitate the use of 4-bit look-up tables which optimizes the resource usage in the Stratix 2 devices. Each 16.5 ns, 140 bits of data are tested for possible matches with a predefined set of patterns and for each pattern, the number of hits that are not present in the input data is counted. Valid track segments correspond to matches in the inner, middle and outer sets of four wires with at most 1, 2 or 3 missed wires. Each matched track segment is indicated by one of 12 bits that subdivide the azimuthal position of each cell. Three copies of these data are sent to Stereo Linker Association Modules via a fiber transmitter mezzanine board. Pixel data with greater precision is made available for transmission to the level 2 trigger upon receipt of a Level 1 accept.

### C. Stereo Linker Association Module

The Stereo Linker Association Modules (SLAM) replace the Linker Output Modules used in the axial XFT system. The SLAM modules receive the list of axial tracks found by the Linker Modules via the crate backplane and the stereo

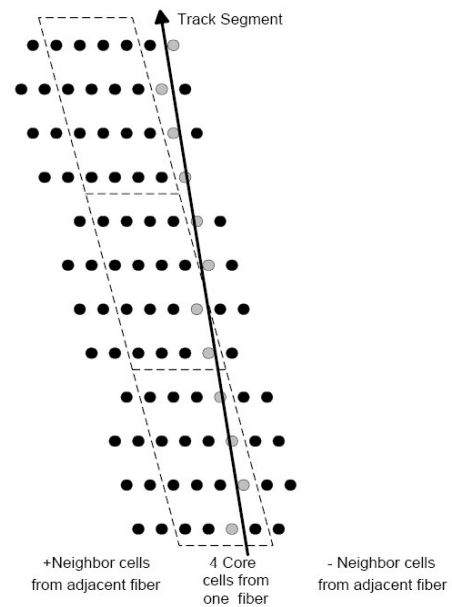


Fig. 5. Stereo finder track segment identification. The number of unmatched bits in three groups of 4 wires are summed to match track segments with at most 1, 2 or 3 misses.

pixel data from the Stereo Finder Modules via fiber receivers on the front panel. Data from the fibers are deserialized using TLK1501 devices and input to a single Altera Stratix I EP1S60 FPGA which performs the association of stereo pixels with axial tracks. The association is made by exploiting the correlation between the azimuthal position of an axial track and the distances to the associated pixels found in the stereo super-layers. Because of the  $\pm 2^\circ$  stereo angle on alternating stereo super-layers, stereo pixels will be alternately offset by up to five cells in the positive and negative direction,

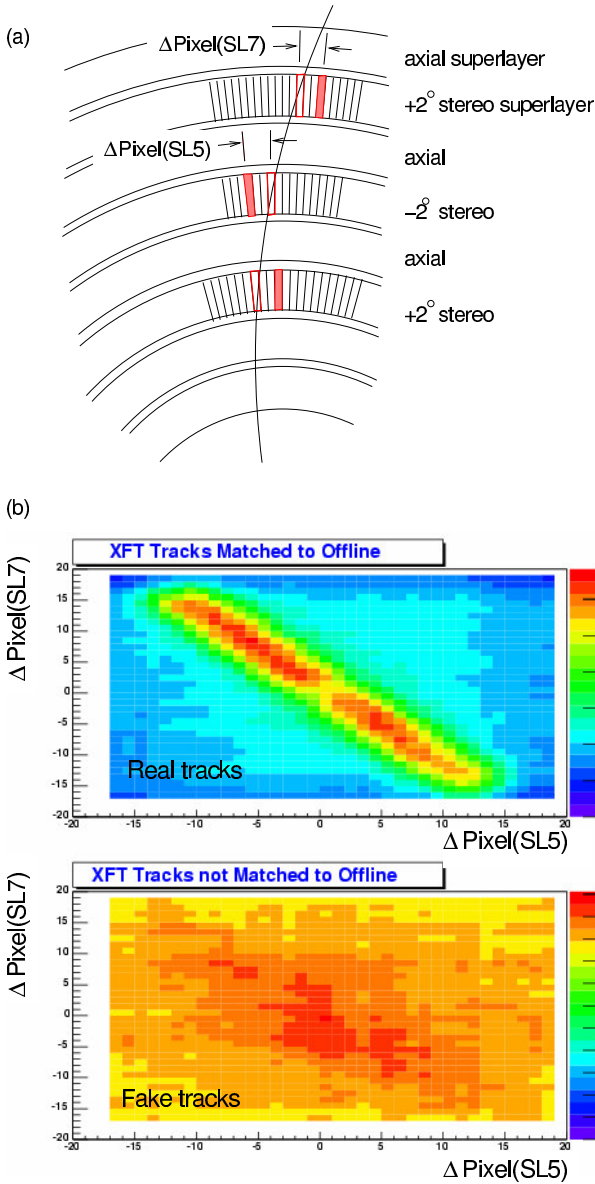


Fig. 6. (a) Displacement of stereo pixels from expected position at  $z = 0$  due to the alternating stereo angle of wire planes. (b) Correlation between the azimuthal positions of stereo pixels in the outer two stereo super-layers and the azimuthal position of the axial track at  $z = 0$ . Axial XFT tracks associated with tracks identified using the full event reconstruction show a strong correlation, while those not associated with reconstructed tracks do not.

depending on the polar angle of the track.

Figure 6 illustrates this correlation for real tracks using two stereo super-layers and shows no significant correlation in the case of fake axial tracks. The logic implemented in the SLAM FPGA maps the input axial track words onto a set of possible pixel positions which are tested against the pixels received from the stereo finder. The Boolean sum of products of these matches represents a match between the axial track and at least one predefined pattern of stereo pixels. The bits in the axial track word that previously indicated track isolation or high rapidity have now been redefined to indicate the confirmation

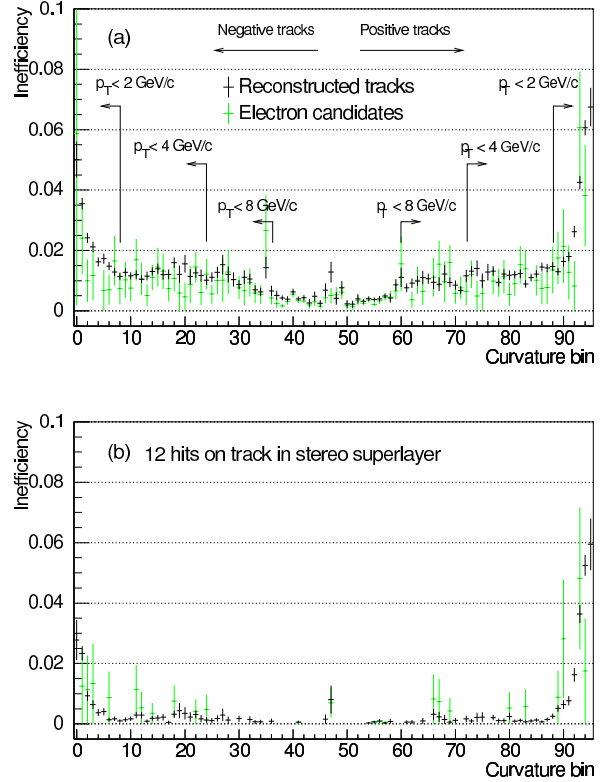


Fig. 7. Pixel inefficiency as a function of XFT track curvature ( $p_T$  bin) for the middle of the three instrumented super-layers. All tracks are considered in (a), while tracks in (b) are required to have 12 associated hits in the super-layer.

status. The resulting track words with the stereo confirmation bits are output via the front panel of the SLAM modules to the XTRP system in the same format provided by the Linker Output Modules.

## V. PERFORMANCE

### A. Stereo Finder Efficiency

The efficiency with which the stereo finder sets the appropriate bit to indicate the presence of a track segment at a particular azimuthal position within a cell has been determined for tracks reconstructed using the full tracking chamber information. This sample of tracks has high purity, but the purity can be increased further by selecting electron candidates, requiring that they point to clusters of energy in the electromagnetic calorimeter. Figure 7 shows the inefficiency for identifying pixels on one of the stereo super-layers as a function of track curvature. In this case, pixels were required to have at least 11 out of 12 wires match the patterns defined in the Stereo Linker logic. Much of the inefficiency is due to the chamber single hit inefficiency – requiring the reconstructed track to have 12 hits associated with it in the super-layer in question reduces the Stereo Finder inefficiency to less than 1% when  $p_T > 2 \text{ GeV}/c$ . Some of the structure seen in Figure 7(a) is due to a trigger bias which enriches the fraction

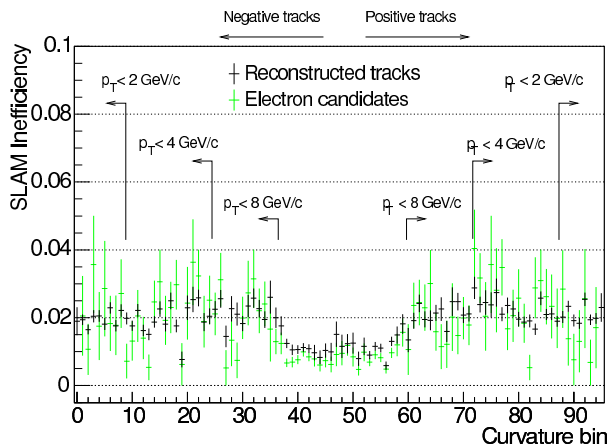


Fig. 8. Inefficiency for association stereo pixels with axial XFT tracks in cases where the axial track is associated with a reconstructed track and pixels in all three stereo super-layers are found in its vicinity.

of tracks in this sample that are electrons with  $p_T > 8 \text{ GeV}/c$ . High  $p_T$  electrons deposit more ionization in the tracking chamber than do lower momentum pions and leads to an apparent increase in efficiency when  $p_T > 8 \text{ GeV}/c$ . Nevertheless, such analyses demonstrate that any inefficiency caused by lack of pattern coverage is small.

### B. SLAM Efficiency

Since the SLAM requires pixels to be found in each of the three instrumented stereo super-layers, the efficiency with which real tracks found by the axial XFT system are confirmed is dominated by the inefficiencies of the Stereo Finder modules. Figure 8 shows that when pixels are found on all three stereo super-layers in the vicinity of a track, the efficiency for confirming the presence of a real track exceeds 98% over all momenta.

### C. Reduction of Trigger Rates

The CDF II detector is operated at high instantaneous luminosities with the goal of maximizing the efficiency of triggers sensitive to high  $p_T$  processes such as those with intermediate vector bosons in the final state. This mode of operation benefits from the improved track purity provided by the XFT upgrade which is used to control the rates of high  $p_T$  track triggers, providing more optimal use of the available level 1 and level 2 trigger bandwidth. Figure 9 illustrates the trigger rate reduction provided by requiring stereo confirmation on tracks associated with muon stubs in the region of pseudo-rapidity  $0.6 < \eta < 1.0$ . The muon chambers in this region have high occupancies and the trigger rate is dominated by fake tracks found by the axial XFT system extrapolated to uncorrelated muon chamber activity. By requiring stereo confirmation, the rates are reduced by a factor of 4 at high luminosity.

## VI. CONCLUSIONS

The upgrade of the axial XFT trigger system described here was completed in the Fall of 2006 and has been used in the

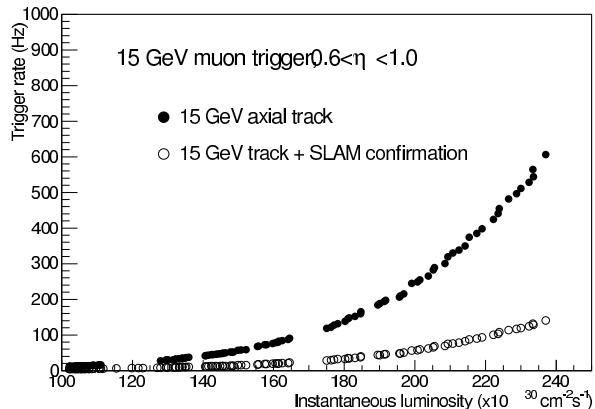


Fig. 9. Trigger rates for muons in CDF with  $0.6 < \eta < 1.0$  associated with at  $15 \text{ GeV}/c$  XFT track.

collection of physics quality data since that time. The only significant interference with the operation of the axial XFT system during data taking occurred with the Linker Output Modules were replaced by the SLAM modules, but these were initially programmed in a way that allowed them to emulate the functionality of the Linker Output Modules.

In addition to improving the purity of axial XFT tracks used in the level 1 trigger, both the Stereo Finder and the SLAM module provide data that can be used by the level 2 trigger system. These provide stereo pixel data to the level 2 trigger processor with greater precision than is available for use in the level 1 trigger. The use of stereo pixels in the level 2 trigger makes possible the implementation of trigger decisions based on limited 3D tracking[9]. The SLAM modules also provides a list of tracks to the level 2 trigger with lower latency than was previous possible via the XTRP system. No further upgrades to the level 1 track trigger hardware are anticipated during the remainder of the Tevatron run.

### ACKNOWLEDGMENT

The author would like to acknowledge work carried out by many contributors to the level 1 track trigger upgrade that has not been explicitly mentioned here. These efforts were essential for the successful design, completion and commissioning of the new hardware, on-line software and diagnostic tools.

### REFERENCES

- [1] E.J.Thomson, *et al.*, IEEE Trans. Nucl. Sci. 49, 1063 (2002).
- [2] T. Affolder, *et al.*, Nucl. Instrum. Meth. A526: 249 (2004).
- [3] B. Ashmanskas, *et al.*, Nucl. Instrum. Meth. A518: 532 (2004).
- [4] A. Abulencia, *et al.*, Phys. Rev. Lett. 97, 242003 (2006).
- [5] "IEEE Standard for a Common Mezzanine Card Family: CMC," Document 1386-2001, ANSI Pub., 2001.
- [6] K. Anikeev, *et al.*, IEEE Trans. Nucl. Sci. TNS-00560-2004.
- [7] Texas Instruments, "TLK1501: 0.6 to 1.5 GBPS Transceiver," Data sheet, 2004.
- [8] Altera Corporation, "Stratix II Device Handbook", August 2006.
- [9] A. Ivanov, these proceedings.